In situ Photoemission Study of the Room Temperature Ferromagnet $ZnGeP_2$:Mn

Y. Ishida,[1] D. D. Sarma,[2,3] K. Okazaki,[1] J. Okabayashi,[1] J. I. Hwang,[3] H. Ott,[4] A. Fujimori,[1,3] G. A. Medvedkin,[5] T. Ishibashi,[5] and K. Sato[5]

[1]*Department of Physics, University of Tokyo, Bunkyo-ku Tokyo 113-0033, Japan*
[2]*Solid State and Structural Chemistry Unit, Indian Institute of Science, Bangalore 560 012, India*
[3]*Department of Complexity Science, University of Tokyo, Bunkyo-ku Tokyo 113-0033, Japan*
[4]*Institut für Experimentalphysik Freie Universität Berlin, Arnimallee 14, 14195 Berlin, Germany*
[5]*Tokyo University of Agriculture and Technology, Koganei, Tokyo 184-8588, Japan*

(Received 20 March 2003; published 5 September 2003)

The chemical states of the $ZnGeP_2$:Mn interface which shows ferromagnetism above room temperature have been studied by photoemission spectroscopy. Mn deposition on the $ZnGeP_2$ substrate heated to 400 °C induced Mn substitution for Zn and then the formation of metallic Mn-Ge-P compounds. Depth profile studies have shown that Mn 3*d* electrons changed their character from itinerant to localized along the depth, and in the deep region, dilute divalent Mn species ($< 5\%$ Mn) was observed with a coexisting metallic Fermi edge of non-Mn 3*d* character. The possibility of hole doping through Mn substitution for Ge and/or Zn vacancy is discussed.

DOI: 10.1103/PhysRevLett.91.107202 PACS numbers: 75.70.Cn, 75.50.Pp, 79.60.Jv

The successful synthesis of the III-V-based ferromagnetic diluted magnetic semiconductors (DMSs) has opened up a number of exciting functionalities such as nonvolatile memories, spin injection, and optical control of ferromagnetism [1]. However, the Curie temperatures (T_C's) of the prototypical $In_{1-x}Mn_xAs$ and $Ga_{1-x}Mn_xAs$ are below 200 K due to the limitation in incorporating Mn ions and *p*-type carriers [2]. The search for new high-T_C DMSs has been a challenging subject [3].

Recently, Medvedkin *et al.* introduced a new class of DMSs, namely, the Mn-doped II-IV-V_2 chalcopyrite semiconductors, which showed ferromagnetism above room temperature (RT) [4,5]. A high concentration of Mn is incorporated into the chalcopyrites by the deposition of Mn metal and annealing. The II-V-V_2 chalcopyrite has two types of cation sites, which allows us to functionalize each cation site in different ways, e.g., isovalent substitution of Mn^{2+} at the II site and acceptor doping at the IV site. This is conceptually different from the III-V-based DMS, where the anisovalent substitution of Mn^{2+} at the III sites acted as both local magnetic moment and acceptor. In addition, the chalcopyrites have many defects, e.g., Zn ion on Ge site (Zn_{Ge}), Zn vacancy (V_{Zn}), etc., in $ZnGeP_2$, which may also act as acceptors [6]. This rich chemistry stimulated many theoretical calculations on II-IV-V_2:Mn [7].

Photoemission spectroscopy (PES) is a powerful tool to investigate the electronic structures of DMSs [8]. Particularly, Mn 3*d* partial density of states (PDOS) is obtained through resonant PES and subsequent analyses provide *p-d* exchange interaction between the Mn 3*d* electrons and the host semiconductor. In the present work, we have studied the depth profile of $ZnGeP_2$:Mn interface and its growth condition by PES. The electronic state of Mn along the depth is studied by Ar^+ sputtering. The depth profile of the magnetization is also provided.

Ultraviolet photoemission (UPS) and x-ray photoemission (XPS) measurements were performed at BL-18A of the Photon Factory. The total energy resolution of the spectrometer including temperature broadening was

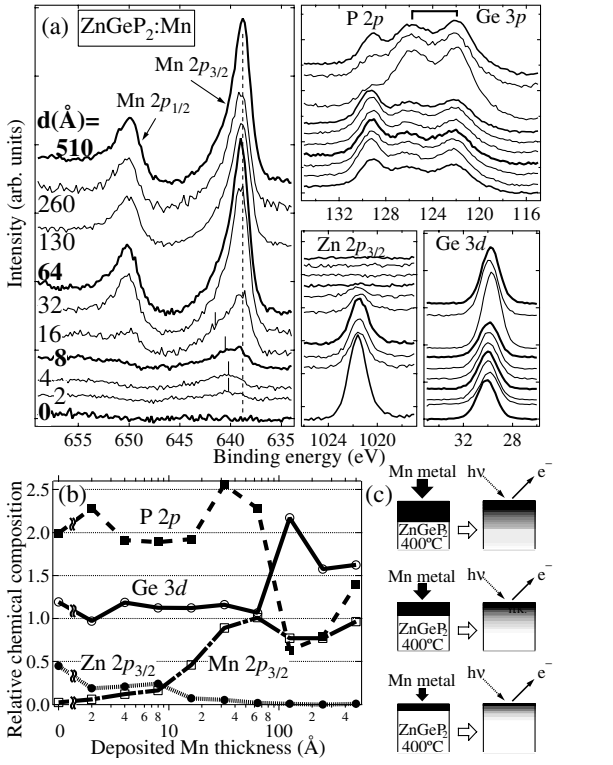

FIG. 1. Core-level spectra of $ZnGeP_2$:Mn for various Mn thicknesses deposited at 400 °C. (a) Raw spectra. The vertical scale is counts per second. The 0 Å corresponds to the sputtered and annealed surface of the $ZnGeP_2$ substrate. (b) Core-level intensities as functions of deposited Mn thickness. For normalization, see text. (c) Schematic description of the Mn deposition.

800 meV for XPS and 200 meV for UPS. The pressure was below 7×10^{-10} Torr during the measurements. A single crystal of $ZnGeP_2$, which had been chemically and mechanically polished [(001) to the surface normal] [5], was loaded into the spectrometer and cleaned by Ar^+-ion sputtering at 1.5 kV. Surface cleanliness was checked by the absence of O 1*s* and C 1*s* contaminations by XPS. Then the substrate was annealed to 400 °C, and Mn metal (99.999%) was deposited at the rate of 3 Å/min [9]. After the Mn deposition, the sample was postannealed for 5 min and then cooled to RT. All the spectra were taken at RT. The Fermi level was calibrated by the Fermi cutoff of the metal in electrical contact with the sample. Ar^+-ion sputtering at 1.5 kV was used for sample etching. The sputter-etching rate was ~2 Å/min. The magnetization was measured *ex situ* using a SQUID magnetometer. For comparison, polycrystalline MnP ($T_C = 290$ K [10]) was also measured.

First, the effect of annealing and sputtering on the $ZnGeP_2$ substrate was studied. The core-level intensities above 300 °C showed strong Zn deficiency and weak Ge excess [see the relative chemical composition at $d = 0$ Å in Fig. 1(b), where the deviation from the stoichiometry of $ZnGeP_2$ is seen once annealed at 400 °C]. Possible dynamics of Mn diffusion at the 400 °C substrate is the migration of Mn atoms through this Zn deficient region. This region could be removed by 3-min Ar^+-ion sputtering (corresponding to ~6 Å thickness). Further sputtering did not change the core-level intensities of the substrate within the accuracy of 3%. This suggests that selective sputtering between Zn, Ge, and P can be ignored. We therefore considered that the spectra of the sputtered surface in the following experiments represent the chemical composition of the $ZnGeP_2$:Mn sample at each point of the depth profile. As for Mn atoms, the selective sputtering effect may be equally small, since the mass of Mn is similar to those of Zn and Ge.

Next we show a series of spectra for Mn deposition on the 400 °C-annealed substrate [Fig. 1(c)]. Each time after having taken a set of spectra for one Mn coverage, the deposited Mn was completely removed by prolonged sputtering and then Mn was newly deposited. Figure 1(a) shows the core-level spectra of the Mn-deposited surface, and Fig. 1(b) shows their intensities normalized to those for the as-sputtered $ZnGeP_2$. The Mn $2p_{3/2}$ intensity has been normalized using the Mn $2p_{3/2}$ and P $2p$ intensity ratio of MnP. In the region of Mn thickness $d < 64$ Å, one can see a monotonic increase and decrease of the Mn and Zn signals, respectively, without significant changes in the Ge and P intensities. This suggests that Mn atoms primarily substituted for Zn and a $Zn_{1-x}Mn_xGeP_2$-like compound was formed. In the Mn $2p_{3/2}$ spectra below $d = 16$ Å, one can see signal on the higher binding energy side [vertical bars in Fig. 1(a)] of the dominant metallic peak ($E_B = 638.7$ eV, broken line). This indicates that a portion of the Mn atoms chemically reacted with the substrate and became Mn^{2+}. In going from $d = 64$ to 130 Å, the Ge and P intensities suddenly changed. The saturation of the Mn intensity with sizable signals of Ge and P above $d = 130$ Å is a signature of atomic diffusion for such a thick Mn overlayer. The surface region above $d = 130$ Å consisted of Ge-rich, ternary metallic compound(s) of Mn, Ge, and P with possible inhomogeneity and/or phase mixture.

The valence-band spectra taken for photon energies in the Mn $3p$-$3d$ core-excitation region are shown in Fig. 2. The spectra have been normalized to the postfocusing Au mirror current and then to the intensities of the $d = 0$ Å spectra at the corresponding photon energies. The Mn $3d$-drived spectra were obtained by subtraction between these normalized on-resonance (51 eV) and off-resonance (48 eV) spectra. In this way, we could virtually eliminate the effect of photon energy dependence of the host valence band. For $d = 4$ and 16 Å, one can see a peak located at $E_B \sim 4$ eV in the difference spectra. This is similar to the previous results of the Mn incorporated II-VI- and III-V-based DMSs [8] and is thus attributed to the localized nature of Mn $3d$ electrons. However, above $d = 32$ Å, there was a change in the decay process of the Mn $3p$ core hole, and a strong Mn $M_3L_{4,5}L_{4,5}$ Auger peak replaced the ~4 eV peak. This indicates that the Mn $3d$ electrons became itinerant. The disappearance of the ~4 eV peak at $d = 32$ Å is in accordance with the Mn $2p$ core-level spectrum [Fig. 1(a)], where the divalent Mn signal disappeared and the asymmetric line shape characteristic of a metallic Mn compound appeared. We note that MnP also shows Mn $M_3L_{4,5}L_{4,5}$ Auger signals in the valence-band spectra [11]. However, the Mn $2p_{3/2}$ core-level peak of MnP was observed at $E_B = 639.2$ eV, different from the peak positions observed above $d = 32$ Å in Fig. 1(a). At $d = 16$ Å both a clear

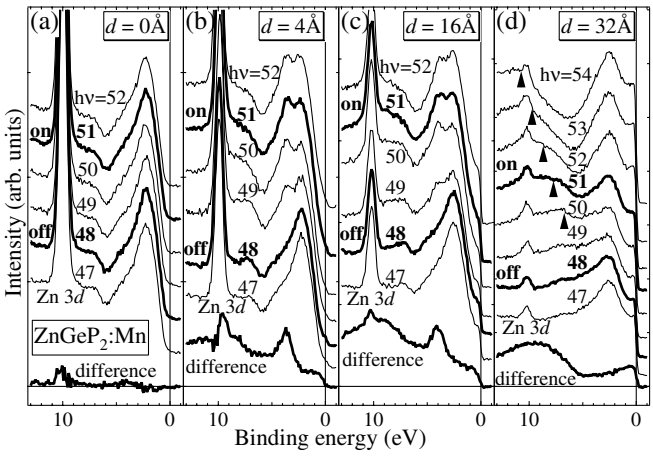

FIG. 2. Valence-band spectra of $ZnGeP_2$:Mn in the $3p$-$3d$ core excitation region. On- and off-resonance energies are 51 and 48 eV, respectively, and the spectra at the bottom show their difference spectra. Triangles in (d) indicate the constant kinetic energy of the Mn $M_3L_{4,5}L_{4,5}$ Auger signal.

Fermi edge and the ~4 eV peak are observed. The difference spectrum at $d = 16$ Å is almost a superposition of the $d = 4$ and 32 Å spectra, as in the case of the Mn $2p$ core-level spectra [Fig. 1(a)].

In order to study the chemical states formed underneath the surface metallic compound(s), $ZnGeP_2$:Mn of the nominal Mn thickness of 150 Å deposited at 400 °C was repeatedly sputter etched without annealing and studied by PES [Fig. 3(c)]. Figure 3(a) shows core-level spectra taken in the sputter-etching series, and Fig. 3(b) shows their intensities. The change in the first 20 min sputtering is attributed to the removal of the metallic Mn-Ge-P (Zn-poor) layer in the surface region. Subsequently, the Mn $2p_{3/2}$ core level started to show a shoulder structure at $E_B = 641.7$ eV due to ionic Mn (Mn^{2+} most likely). The systematic increase of this shoulder and the decrease of the metallic main peak between 20 to 70 min sputtering indicate that these signals are originated from chemically different Mn species. After 100 min sputtering, the relative compositions became Zn:Ge:P ~ 1:1:2, suggesting that the chalcopyrite-type matrix of Zn, Ge, and P plus dilute Mn was exposed [Fig. 3(b)]. After 230 min sputtering, the Mn signal became totally that of the ionic one [Fig. 3(a)], indicating that a dilute-Mn phase (< 5% Mn) appeared. It was difficult to determine from Fig. 3(b) which element Mn substituted for, because Zn:Ge:P ~ 1:1:2 and the amount of Mn was small.

Figure 4 shows the valence-band spectra in the sputter-etching series for photon energies in the Mn $3p$-$3d$ core-excitation region. Before 80 min sputtering, the $M_3L_{4,5}L_{4,5}$ Auger process was dominant [Fig. 4(a) and 4(b)], and after that resonant photoemission became dominant [Fig. 4(c) and 4(d)]. This indicates again that the Mn $3d$ states changed their character from itinerant to localized along the depth. A peak at $E_B \sim 4$ eV was seen after 80 min sputtering, and hence Mn was divalent in the deep region. The divalent Mn signal in the recent EPR measurements may come from this region [12]. The Mn $3d$-derived intensity near E_F in the difference spectra is weak compared to that in Fig. 2(b). This indicates that the Mn $3d$ states are more localized in the deep bulk region than the $Zn_{1-x}Mn_xGeP_2$-like phase in the early stage of Mn deposition. The inset of Fig. 4 shows valence-band spectra near E_F after 230 min sputtering. They clearly show Fermi edges. Since the Mn $3d$ PDOS is suppressed near E_F, these Fermi edges come from the valence band of the host semiconductor which was somehow doped with metallic charge carriers. Since isovalent substitution of Mn^{2+} for Zn^{2+} cannot produce carriers, Mn^{2+} may have substituted for the Ge site and/or Mn incorporation simultaneously induced defects such as V_{Zn} and Zn_{Ge} which produce hole carriers. The Fermi edge became obscure after 540 min sputtering in accordance with the diminishing Mn $2p$ core-level intensity (Fig. 3). In the sputter-etching series, too, no MnP signal was observed.

We have also studied the depth profile of $ZnGeP_2$:Mn of the 200 Å nominal thickness Mn annealed at 200 °C. Up to 800 min sputtering, the Mn signal was observed together with Zn, Ge, and P signals, indicating the diffusive reaction of Mn into the substrate already at 200 °C.

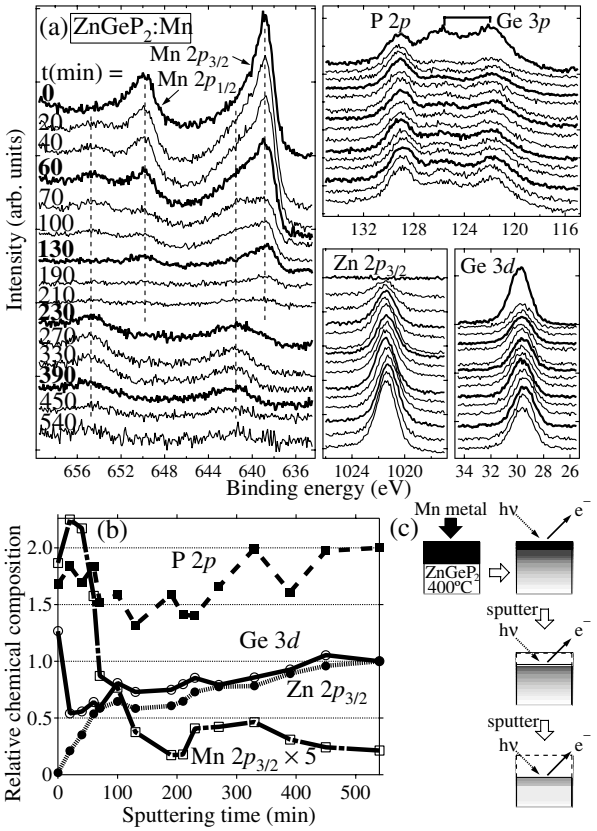

FIG. 3. Core-level spectra of $ZnGeP_2$:Mn in the depth profile. (a) Raw spectra. The vertical scale is counts per second. (b) Core-level intensities as functions to sputtering time. (c) Schematic description of the sputtering series.

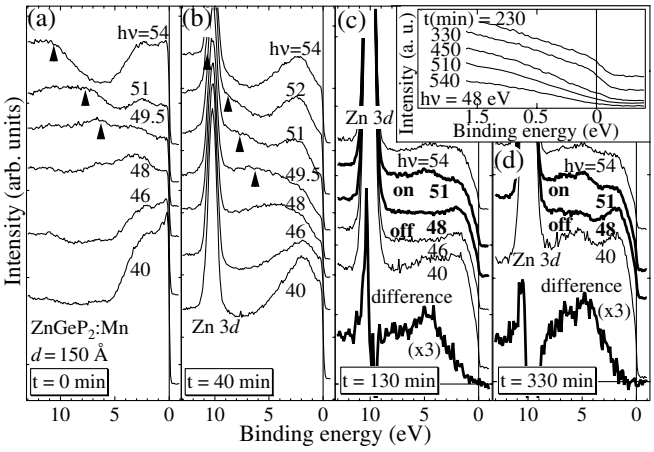

FIG. 4. Valence-band spectra of $ZnGeP_2$:Mn ($d = 150$ Å) in the sputter-etching series. Triangles in (a) and (b) denote the $M_3L_{4,5}L_{4,5}$ Auger signals. The inset shows the valence-band spectra near E_F for sputtering time longer than 230 min.

However, the Mn $2p_{3/2}$ signal always appeared at $E_B = 638.7$ eV without any divalent signal. Correspondingly, only the Mn $M_3L_{4,5}L_{4,5}$ Auger peak was observed in the valence-band spectra. We therefore conclude that the annealing at 200 °C was insufficient for the Mn atoms to be chemically incorporated in the host semiconductor as divalent ions.

Figure 5(a) shows the magnetization of as-prepared $ZnGeP_2$:Mn ($d = 150$ Å at 400 °C) and that after 200 min sputtering. Clear hysteresis was observed at both 10 and 330 K for the 150 Å deposited sample [Fig. 5(a), upper panel]. Surprisingly, the magnetization diminished by only ~10% after removing the surface metallic Mn compound [Fig. 5(a), lower panel]. This indicates that the divalent Mn phase deep in the substrate (< 5% Mn) was a RT ferromagnet. Figure 5(b) clearly shows ferromagnetism up to ~400 K. One can see a kink at ~300 K which may correspond to the $T_C = 312$ K of bulk $Zn_{1-x}Mn_xGeP_2$ [13]. Another anomaly at 20–50 K may also correspond to the 47 K anomaly of bulk $Zn_{1-x}Mn_xGeP_2$. Therefore, the present sample may contain $Zn_{1-x}Mn_xGeP_2$ as a minority phase. Recently, $ZnGeP_2$:Mn interface prepared at 550 °C was studied, and the $M(T)$ curve showed pronounced singularities at ~318 K and 20–50 K and small magnetization tailing above 318 K [14]. This behavior is more similar to bulk $Zn_{1-x}Mn_xGeP_2$ than the present sample. We note that bulk $Zn_{1-x}Mn_xGeP_2$ was reported to be electrically insulating, while the present sample showed a metallic Fermi edge. Further studies are necessary, in particular to understand the relationship between the magnetic behavior, the carrier density, and the preparation temperature.

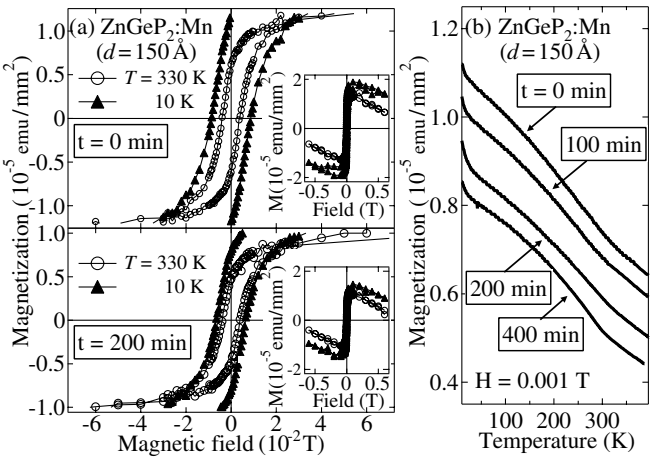

FIG. 5. Magnetization per sample area of $ZnGeP_2$:Mn ($d = 150$ Å) prepared at 400 °C. (a) Magnetization curves at $T = 10$ and 330 K of as-prepared $ZnGeP_2$:Mn (upper) and those after having removed the surface metallic Mn compound (lower). From these data, magnetization per Mn atom is estimated to be $\sim 1.5\mu_B$. Insets show the plots in a wider field range. (b) Magnetization versus temperature in the sputtering series.

In conclusion, we have observed spectral features of localized, most likely divalent Mn 3*d* states incorporated into the host $ZnGeP_2$ in the thin Mn-deposited surface region (probably as a $Zn_{1-x}Mn_xGeP_2$) and in a deep region below the surface metallic Mn compound after thick Mn deposition. A Fermi edge was observed in the deep region, indicating that carrier doping took place in that region of $ZnGeP_2$:Mn. RT ferromagnetism was observed after removing the surface Mn compound. This indicates that ferromagnetism in $ZnGeP_2$:Mn is caused by the dilute-Mn ions in the deep region.

We thank T. Okuda, A. Harasawa, and T. Kinoshita for their technical help, V. G. Voevodin, K. Ono, T. Komatsubara, and M. Okusawa for providing samples, and T. Mizokawa for useful discussions. This work was supported by a Grant-in-Aid for Scientific Research in Priority Area "Semiconductor Spintronics" (No. 14076209) from the MEXT, Japan. D. D. S. thanks the University of Tokyo for hospitality during a part of this work. The experiment was approved by the Photon Factory Program Advisory Committee (Proposal No. 01U005).

[1] H. Ohno, F. Matsukura, and Y. Ohno, JSAP International No. 5, 4 (2002), and references therein.
[2] T. Dietl *et al.*, Science **287**, 1019 (2000).
[3] K. Ueda, H. Tabata, and T. Kawai, Appl. Phys. Lett. **79**, 988 (2001); H. Saeki, H. Tabata, and T. Kawai, Solid State Commun. **120**, 439 (2001); Y. Matsumoto *et al.*, Jpn. J. Appl. Phys. **40**, L1204 (2001); H. Saito *et al.*, Phys. Rev. Lett. **90**, 207202 (2003).
[4] G. A. Medvedkin *et al.*, Jpn. J. Appl. Phys. **39**, L949 (2000); K. Sato *et al.*, J. Appl. Phys. **89**, 7027 (2001).
[5] G. A. Medvedkin *et al.*, J. Cryst. Growth **236**, 609 (2002); K. Sato, G. A. Medvedkin, and T. Ishibashi, J. Cryst. Growth **237–239**, 1363 (2002).
[6] S. D. Setzler *et al.*, J. Appl. Phys. **86**, 6677 (1999).
[7] P. Mahadevan and A. Zunger, Phys. Rev. Lett. **88**, 047205 (2002); Y.-J. Zhao *et al.*, Phys. Rev. B **63**, 201202 (2001); Y.-J. Zhao *et al.*, Phys. Rev. B **65**, 094415 (2002); T. Kamatani and H. Akai, Phase Transit. **76**, 401 (2003).
[8] L. Ley *et al.*, Phys. Rev. B **35**, 2839 (1987); J. Okabayashi *et al.*, Phys. Rev. B **59**, R2486 (1999); J. Okabayashi *et al.*, Phys. Rev. B **65**, R161203 (2002).
[9] We could not observe LEED patterns before and after the sample synthesis.
[10] E. E. Huber, Jr. and D. H. Ridgley, Phys. Rev. **135**, A1033 (1964).
[11] A. Kakizaki *et al.*, J. Phys. Soc. Jpn. **49**, 2183 (1980).
[12] P. G. Baranov *et al.*, J. Supercond. **16**, 131 (2003).
[13] S. Cho *et al.*, Phys. Rev. Lett. **88**, 257203 (2002).
[14] G. A. Medvedkin, P. G. Baranov, and S. I. Goloshchapov, J. Phys. Chem. Solids (to be published).